Analytic Approach to Nonlinear Rayleigh-Taylor and Richtmyer-Meshkov Instabilities

Karnig O. Mikaelian
University of California, Lawrence Livermore National Laboratory,
Livermore, California 94550
(Received 19 August 1996)

We present analytic formulas for the nonlinear evolution of the bubble amplitude in Rayleigh-Taylor and Richtmyer-Meshkov instabilities in two and three dimensions. Direct numerical simulations of He/Xe shock tube experiments are also presented and the results are found to agree well with the analytic formulas which are based on an extension of Layzer's theory [Astrophys. J. **122**, 1 (1955)]. [S0031-9007(97)05039-4]

PACS numbers: 47.20.–k, 52.35.Py

The Rayleigh-Taylor (RT) instability occurs when a heavy fluid is supported by a lighter fluid. It controls astrophysical, geophysical, and industrial processes such as supernova explosions, the formation of salt domes, and the implosion of inertial-confinement-fusion (ICF) capsules. The Richtmyer-Meshkov (RM) instability occurs when a shock crosses an interface between two fluids, and has equally wide applications [1].

The linear regime is well understood. The nonlinear regime is usually treated by numerical simulations [1,2] or high-order expansion of the fluid equations [3,4]. The purpose of this Letter is to present analytic formulas for the evolution of RT and RM instabilities from the linear to the nonlinear regime. We find that these formulas compare well with previous numerical results [1–4], agree with known asymptotic properties of such flows [5,6], and predict new ones. We also present direct numerical simulations for new shock tube experiments and compare the numerical results with our analytic formulas.

Our starting point is Layzer's theory [7]. This theory has been used previously [2,8] but, as far as we know, has not been solved analytically. The theory applies to the bubble amplitude, which we denote by $\eta(t)$. Given the initial amplitude η_0 and its initial growth rate $\dot{\eta}_0$, we find $\eta(t)$ for RT and RM instabilities, treating the latter as an impulsive acceleration, as was done first by Richtmyer [9] and is common practice [1–3].

Layzer treated the RT problem assuming $\eta_0 = 0$. We extended his theory to $\eta_0 \neq 0$ for two purposes: first, to see if and how memory of initial conditions is lost in the nonlinear regime, as the asymptotic properties mentioned above appear to be independent of η_0 and $\dot{\eta}_0$; second, to apply his theory to the RM instability, one needs a finite η_0 because, in this case, $\dot{\eta}_0 \propto \eta_0$ and, indeed, RM simulations and experiments start with $\eta_0 \neq 0$.

We will treat in parallel 2D and 3D geometries considered by Layzer in reverse order. In the first and much more commonly considered geometry [1–5,9], the flow is between two "parallel walls" separated by a distance λ. In the second geometry, also called "tubular flow" (see Fig. 1 in [7]), a bubble rises in a tube of radius R. Hence, the surface of the fluid is given initially by

$$y_0(x_0) = \eta_0 \cos(kx_0) \tag{1a}$$

and

$$z_0(r_0) = \eta_0 J_0(\beta_1 r_0/R)\,, \tag{1b}$$

for 2D and 3D, respectively. Except for J_0, which is the Bessel function of order zero, the zero subscript denotes $t = 0$ values; y and x refer to the vertical and horizontal coordinates, and similarly for z and r. Here, $k = 2\pi/\lambda$ and $\beta_1 \approx 3.832$, the first zero of the Bessel function of order one.

Rayleigh-Taylor.—Our procedure is the same as Layzer's: Assume that, in the neighborhood of the bubble, the velocity potential [Eq. (11) in [7]] satisfies the Bernoulli equation [Eq. (10) in [7]] for 3D flow, similarly for 2D. For $\eta_0 = 0$, Layzer obtained the second order nonlinear differential equation for the all-important function $T(t)$, which determines $\eta(t)$. [There are misprints in Layzer's Eqs. (27) and (28).] For $\eta_0 \neq 0$, we find

$$\theta(2\theta^3 + 1 - 3\eta_0 k)\ddot{\theta} + (\theta^3 - 1 + 3\eta_0 k)\dot{\theta}^2 - gk\theta^2(\theta^3 - 1 + 3\eta_0 k) = 0\,, \tag{2a}$$

$$\theta(\theta^2 + 1 - 2\eta_0\beta_1/R)\ddot{\theta} - (1 - 2\eta_0\beta_1/R)\dot{\theta}^2 - (g\beta_1/R)\theta^2(\theta^2 - 1 + 2\eta_0\beta_1/R) = 0\,, \tag{2b}$$

for 2D and 3D, respectively. The function $\theta(t)$ is defined as $\theta = e^{(\eta-\eta_0)k}$ and $\theta = e^{(\eta-\eta_0)\beta_1/R}$ and is related to Layzer's $T(t)$ via $\theta = 1 + (T - 1)e^{-\eta_0 k}$ and $\theta = 1 + (T - 1)e^{-\eta_0\beta_1/R}$ for 2D and 3D, respectively. As a check, for $\eta_0 = 0$, we have $\theta = T$ and Eqs. (2a) and (2b) reduce to Layzer's Eqs. (55) and (32), respectively.

Despite their nonlinear nature, Eqs. (2a) and (2b) can be integrated to reveal the existence of a conserved quantity,

 0031-9007/98/80(3)/508(4)$15.00

which we denote by E. We find

$$\dot{\theta}^2[\theta + (1 - 3\eta_0 k)/2\theta^2] - gk[\theta^3/3 - (1 - 3\eta_0 k)\ln\theta] = E\,, \tag{3a}$$

$$\dot{\theta}^2[1 + (1 - 2\eta_0\beta_1/R)/\theta^2] - (g\beta_1/R)[\theta^2 - 2(1 - 2\eta_0\beta_1/R)\ln\theta] = E\,. \tag{3b}$$

Equation (2) follows from conservation of E ($dE/dt = 0$). E should not be taken as the energy of the system, although Eq. (3b) with $\eta_0 = R/2\beta_1$ suggests the energy of a harmonic oscillator with a negative "spring constant." For $\eta_0 = 0$, E coincides with the constant found by Layzer [see his Eq. (46)]. In general, E is determined by the initial data

$$E/gk = 3(\dot{\eta}_0)^2(1 - \eta_0 k)k/2g - \tfrac{1}{3}\,, \tag{4a}$$

$$ER/g\beta_1 = 2(\dot{\eta}_0)^2(1 - \eta_0\beta_1/R)\beta_1/gR - 1\,. \tag{4b}$$

We have achieved our first purpose—how the asymptotic bubble velocity, which we denote by $\dot{\eta}_\infty$, is approached starting from arbitrary initial conditions η_0 and $\dot{\eta}_0$: Using the definitions for θ, Eqs. (3a) and (3b) read

$$\dot{\eta} = (g/3k)^{1/2}\left[\frac{e^{3(\eta-\eta_0)k} - 3(1 - 3\eta_0 k)(\eta - \eta_0)k + 3E/gk}{e^{3(\eta-\eta_0)k} + \frac{1}{2} - 3\eta_0 k/2}\right]^{1/2}, \tag{5a}$$

$$\dot{\eta} = (gR/\beta_1)^{1/2}\left[\frac{e^{2(\eta-\eta_0)\beta_1/R} - 2(1 - 2\eta_0\beta_1/R)(\eta - \eta_0)\beta_1/R + ER/g\beta_1}{e^{2(\eta-\eta_0)\beta_1/R} + 1 - 2\eta_0\beta_1/R}\right]^{1/2}. \tag{5b}$$

As η grows $\dot{\eta} \to \dot{\eta}_\infty$ given by

$$\dot{\eta}_\infty = (g/3k)^{1/2}, \tag{6a}$$

$$\dot{\eta}_\infty = (gR/\beta_1)^{1/2}, \tag{6b}$$

as found by Layzer [7] (he identified k with π/R—see below).

To find $\eta(t)$ for any time t, one must integrate Eq. (5). Although this task is simplified considerably by the fact that the right-hand sides of these equations are functions of η only, so that the problem reduces to a simple quadrature, the integrals cannot be performed analytically and one must resort to numerical integration, as Layzer did for $\eta_0 = 0$.

Except for the cases when $\eta_0 = \frac{1}{3}k$ or $R/2\beta_1$ for 2D or 3D flow, when the equations simplify so much that a completely analytic answer is obtained:

$$\eta k = \eta_0 k + (\tfrac{2}{3})\ln\{\cosh[(3gk)^{1/2}t/2] + (\dot{\eta}_0/\dot{\eta}_\infty)\sinh[(3gk)^{1/2}t/2]\}, \tag{7a}$$

$$\eta\beta_1/R = \eta_0\beta_1/R + \ln\{\cosh[(g\beta_1/R)^{1/2}t] + (\dot{\eta}_0/\dot{\eta}_\infty)\sinh[(g\beta_1/R)^{1/2}t]\}, \tag{7b}$$

where $\eta_0 k = \frac{1}{3}$ and $\eta_0\beta_1/R = \frac{1}{2}$, with asymptotic velocities $\dot{\eta}_\infty$ as defined in Eqs. (6a) and (6b) for 2D and 3D flow, respectively.

We have used Eq. (7) to check our numerical integration of Eq. (5). Although Eqs. (7a) and (7b) apply for specific values of η_0 (there are no constraints on $\dot{\eta}_0$), we have found that they also describe well the numerical results for other values of η_0 also. For example, if $\dot{\eta}_0$ is less (greater) than $\dot{\eta}_\infty$, then $\dot{\eta}$ increases (decreases) towards $\dot{\eta}_\infty$. If $\dot{\eta}_0 = \dot{\eta}_\infty$, then Eq. (7) predicts that

$$\eta = \eta_0 + \dot{\eta}_0 t = \eta_0 + \dot{\eta}_\infty t\,, \tag{8}$$

and this is also what we find by numerical integration of Eq. (5). In other words, if the initial growth rate equals the terminal velocity, then the perturbation grows linearly with time in the case of the RT instability. Of course, one way to achieve large initial $\dot{\eta}_0$ is to start with a shock followed by a constant acceleration, a situation quite common in ICF implosions.

Richtmyer-Meshkov.—Taking $t = 0$ as the shock arrival time and Δv as the jump velocity induced by the shock, we let $g \to \Delta v\,\delta(t)$ in the Bernoulli equations. Richtmyer [9] initiated this incompressible approach and found that compressible effects could be summed up as a simple prescription to use post-shock densities and amplitudes. Although there are subtle exceptions to this prescription [10], one finds that it works in practically all cases [1,9–11].

In this way, we find

$$\dot{\eta}_0 = \Delta v\, k\, \eta_0\,, \tag{9a}$$

$$\dot{\eta}_0 = \Delta v\, \beta_1 \eta_0/R\,, \tag{9b}$$

for 2D and 3D, respectively. Equation (9a) agrees with Richtmyer's result $\dot{\eta}_0 = \Delta v k A \eta_0$ (note that we are considering the case $A = 1$, where A is the Atwood number). It is possible to ignore Eq. (9) and initiate a problem with $\eta_0 = 0$ and some arbitrary $\dot{\eta}_0$ (this was done, for example, in Ref. [2]), but in real applications the perturbation is seeded by a finite η_0. For example, to initiate the RT problem discussed earlier with $\dot{\eta}_0 = \dot{\eta}_\infty$, use a shock $\Delta v = (\frac{g}{3})^{1/2}/\eta_0 k^{3/2}$ to impart the needed terminal velocity from the beginning. As we saw in Eq. (8), the subsequent acceleration will keep η growing linearly with time. Without that acceleration, η will slow down and grow only logarithmically with time, as we will see below.

After the passage of the shock, the evolution equations are the same as in the RT case with $g = 0$. Equations (2a) and (2b) can now be solved analytically and, for the 2D case, we find

$$\eta k = \eta_0 k + (\tfrac{2}{3})\ln(1 + 3\dot{\eta}_0 kt/2), \qquad \eta_0 k = \tfrac{1}{3}, \tag{10}$$

$$3Y_0\dot{\eta}_0 kt/2 = Y - Y_0 + (b^{1/2}/2)\ln\left[\frac{(Y - b^{1/2})(Y_0 + b^{1/2})}{(Y + b^{1/2})(Y_0 - b^{1/2})}\right], \qquad \eta_0 k < \tfrac{1}{3}, \tag{11}$$

$$3Y_0\dot{\eta}_0 kt/2 = Y - Y_0 + \sqrt{-b}\,[\arctan(Y_0/\sqrt{-b}\,) - \arctan(Y/\sqrt{-b}\,)], \qquad \eta_0 k > \tfrac{1}{3}. \tag{12}$$

Here, $Y_0 = \sqrt{3(1 - \eta_0 k)/2}$, $b = (1 - 3\eta_0 k)/2$, and Y is defined by $Y^2 = \theta^3 + b = e^{3(\eta - \eta_0)k} + \frac{1}{2} - 3\eta_0 k/2$.

For 3D flow, we find

$$\eta\beta_1/R = \eta_0\beta_1/R + \ln(1 + \beta_1\dot{\eta}_0 t/R), \qquad \eta_0\beta_1/R = \tfrac{1}{2}, \tag{13}$$

$$Y_0\dot{\eta}_0\beta_1 t/R = Y - Y_0 + b^{1/2}\ln\left[\frac{\theta(Y_0 + b^{1/2})}{Y + b^{1/2}}\right], \qquad \eta_0\beta_1/R < \tfrac{1}{2}, \tag{14}$$

$$Y_0\dot{\eta}_0\beta_1 t/R = Y - Y_0 + \sqrt{-b}\,[\arccos(\sqrt{-b}\,) - \arccos(\sqrt{-b}/\theta)], \qquad \eta_0\beta_1/R > \tfrac{1}{2}. \tag{15}$$

Here, $Y_0 = \sqrt{2(1 - \eta_0\beta_1/R)}$, $b = 1 - 2\eta_0\beta_1/R$, and Y is defined by $Y^2 = \theta^2 + b = e^{2(\eta - \eta_0)\beta_1/R} + 1 - 2\eta_0\beta_1/R$. As in the RT case, we find that Eqs. (10) and (13) are good representatives for other values of η_0 also.

The asymptotic velocities can be obtained directly from Eq. (3):

$$\dot{\eta}_\infty = 2/3kt, \tag{16a}$$

$$\dot{\eta}_\infty = R/\beta_1 t, \tag{16b}$$

for 2D and 3D, respectively, and are independent of η_0 and $\dot{\eta}_0$.

In Layzer's theory, the surface of the fluid is effectively represented by a quadratic function near the tip of the bubble and higher-order terms are neglected. This expansion yields accurate results for the asymptotic bubble velocity $\dot{\eta}_\infty$ because in steady state the bubble is round and the higher-order terms vanish. At intermediate times, however, this approximation may overestimate the transient velocity $\dot{\eta}$.

Comparing 2D and 3D geometries, we find $\dot{\eta}_\infty(3\mathrm{D})/\dot{\eta}_\infty(2\mathrm{D}) = (3kR/\beta_1)^{1/2}$ and $3kR/2\beta_1$ for RT and RM, respectively. If we identify kR with π, we get $\sqrt{3\pi/\beta_1} \approx 1.6$ and $3\pi/2\beta_1 \approx 1.2$, respectively. If we identify kR with β_1, we get $\sqrt{3} \approx 1.7$ and 1.5, respectively. The first identification, adopted by Layzer, is perhaps more physical (the radius of the tube is half the distance between the parallel walls), while the second identification yields equal initial growth rates [see Eq. (9)]. In either case, the ratio is larger for RT than for RM. The RT ratio quoted in Ref. [6] is 1.6. We know of no other investigation into the RM ratio.

We now turn to earlier calculations of the 2D RM bubble velocity, where completely different methods were used. In Ref. [2], Layzer's equations with $\eta_0 = 0$ were integrated numerically, so we expect, and indeed find, that our analytic formulas show very good agreement with their result. (See Fig. 1 in Ref. [2]. We suspect that the scale $\lambda = 2$ in that figure caption must read $\lambda = 1$.) More interesting are the direct numerical simulations with incompressible fluids reported in Ref. [2], which agree quite well with their numerical integration of Layzer's

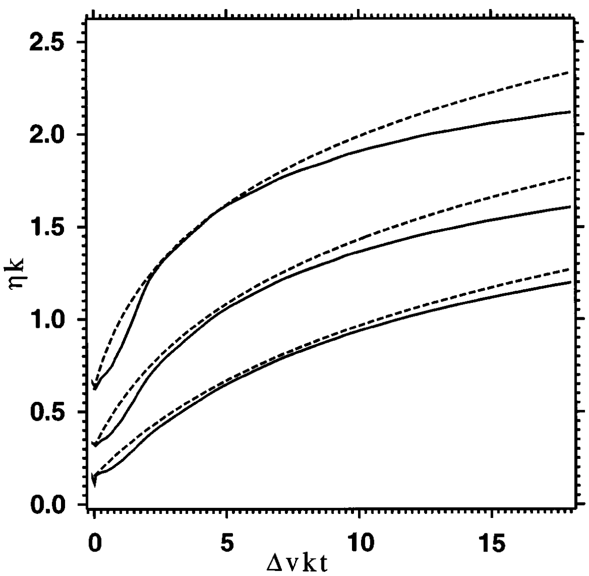

FIG. 1. ηk as a function of $\Delta v kt$ for $\eta_0 k = \frac{1}{6}$, $\frac{1}{3}$, and $\frac{2}{3}$. The continuous curves are from direct numerical simulations with $\eta_0 = 0.35$, 0.70, and 1.40 cm, $k = 2\pi/13\ \mathrm{cm}^{-1}$. A Mach 1.2 shock traveling at $W_i \approx 121$ cm/ms in helium strikes a He/Xe interface (an example is shown in Fig. 2) giving $\Delta v \approx 8.25$ cm/ms. The dashed curves are from Eqs. (10)–(12). We have used Richtmyer's prescription $\dot{\eta}_0 = \Delta v k A_{\mathrm{after}}\eta_{\mathrm{after}}$ with $A_{\mathrm{after}} = 0.94$ (this is also A_{before}, the He and Xe get compressed by the same amount) and $\eta_{\mathrm{after}} = (1 - \Delta v/W_i)\eta_0 \approx 0.93\eta_0$.

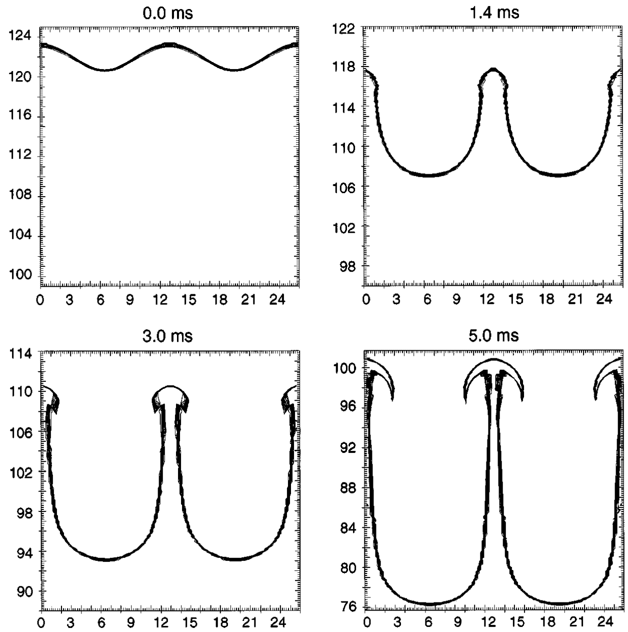

FIG. 2. Isodensity contours from a Mach 1.2 He/Xe simulation with perturbations of $\eta_0 = 1.40$ cm and $\lambda = 13$ cm. The 26 cm $\times$ 26 cm frames move down with the interface located initially at $y = 122$ cm. The bubble vertex is well described by $y(x = 6.5 \text{ or } 19.5, t) = 122 - 8.25t - \eta(t)$, where all dimensions are in cm, t is in ms, and $\eta(t)$ is given by Eq. (12).

equations and, in turn, with our analytic result. In fact, using Eq. (10), we find

$$\dot{\eta}(t) = \frac{\dot{\eta}_0}{1 + 3\dot{\eta}_0 kt/2}, \qquad (17)$$

which automatically gives the correct $\dot{\eta}_0$ and $\dot{\eta}_\infty$ $(=2/3kt)$. For intermediate values of t, say $t = 1$, Eq. (17) gives 0.07 (set $\dot{\eta}_0 = 0.2$ and $k = 2\pi$), which agrees very well with Fig. 1 in Ref. [2].

A completely different technique (Padé approximants) was used in Ref. [3]. The resulting analytic expressions are presumably too long and have not appeared in the literature. Nevertheless, their numerical results for the bubble velocity given in their Fig. 3 agree very well with the expression $\Gamma = 1/(1 + 3\tau/2)$, which follows from Eq. (17). For example, at $\tau = \frac{3}{2}$ we find $\Gamma = \frac{4}{13} \approx 0.3$, in good agreement with Ref. [3].

A different result was reached in Ref. [12]: $\dot{\eta}_\infty$ depends on η_0. This was based on first and second order Padé approximants and, presumably, the results of Ref. [3] based on a tenth order Padé approximant are more accurate. For example, the lowest-order result from Ref. [12] is $\dot{\eta}_\infty = P_1^0 = 1/\eta_0 k^2 t$. It is possible, of course, that memory of initial conditions is lost as higher- and higher-order terms are included in the approximation.

Equations (10)–(12) are plotted in Fig. 1 for $\eta_0 k = \frac{1}{6}$, $\frac{1}{3}$, and $\frac{2}{3}$. Equation (10) is an equally good representation for all three curves, differing by no more than 10% from the exact results. For each value of k, we also plot the results of direct numerical simulations with the fully compressible hydrocode CALE. We chose perturbations of $\lambda = 13$ cm and $\eta_0 = 0.35$, 0.7, and 1.4 cm at the interface between helium ($\rho = 0.17$ mg/cm^3, $\gamma = \frac{5}{3}$) and xenon ($\rho = 5.4$ mg/cm^3, $\gamma = \frac{5}{3}$) which have an Atwood number of 0.94. A Mach 1.2 shock directed from He to Xe induces a $\Delta v \approx 8.25$ cm/ms. These parameters were chosen from Cal Tech's 17 in. shock tube with a 122 cm long test section which is about twice the recently reported value [13]. The extra length allows us to view the interface over a longer period of time without interference from a reflected shock and, thus, follow the evolution from the linear to the nonlinear regime.

Figure 1 shows good agreement between Eqs. (10)–(12) and the direct numerical simulations. Snapshots of the large-amplitude run, $\eta_0 = 1.4$ cm, are shown in Fig. 2. Many features of the interface, particularly the mushrooming spikes, are beyond the scope of Layzer's theory. What we have shown is that his theory, generalized to $\eta_0 \neq 0$ and applied to the RM instability, can be solved analytically and captures well the motion of the bubble vertex from the linear to the nonlinear regime.

This work was performed under the auspices of the U.S. Department of Energy by the Lawrence Livermore Laboratory under Contract No. W-7405-ENG-48.

[1] D. H. Sharp, Physica (Amsterdam) **12D**, 3 (1984). Recent developments are reported in the Proceedings of the 5th International Workshop on the Physics of Compressible Turbulent Mixing (to be published).

[2] J. Hecht, U. Alon, and D. Shvarts, Phys. Fluids **6**, 4019 (1994).

[3] A. L. Velikovich and G. Dimonte, Phys. Rev. Lett. **76**, 3112 (1996).

[4] G. Hazak, Phys. Rev. Lett. **76**, 4167 (1996).

[5] G. Birkhoff and D. Carter, J. Math. Mech. **6**, 769 (1957).

[6] N. A. Inogamov and S. I. Abarzhi, Physica (Amsterdam) **87D**, 339 (1995).

[7] D. Layzer, Astrophys. J. **122**, 1 (1955).

[8] H. J. Kull, Phys. Rev. A **33**, 1957 (1986).

[9] R. D. Richtmyer, Commun. Pure Appl. Math. **13**, 297 (1960).

[10] K. O. Mikaelian, Phys. Rev. Lett. **71**, 2903 (1993); Phys. Fluids **6**, 536 (1994).

[11] Y. Yang, Q. Zhang, and D. H. Sharp, Phys. Fluids **6**, 1856 (1994).

[12] Q. Zhang and S.-I. Sohn, Phys. Lett. A **212**, 149 (1996).

[13] M. Vetter and B. Sturtevant, Shock Waves **4**, 247 (1995).